COMMUNICATIONS TO THE EDITOR

Laminar Flows in Inlet Sections of Tubes and Ducts

F. W. SCHMIDT and B. ZELDIN

The Pennsylvania State University, University Park, Pennsylvania

As a fluid flows through a tube or duct its velocity profile undergoes a change from its initial entrance form to that of a fully developed profile at an axial location far downstream from the entrance. A variety of methods have been employed for the determination of the flow characteristics in this region. An overwhelming majority of these methods employ the boundary layer assumptions thus neglecting the axial transport of vorticity and assuming that pressure is a function of axial distance only. Difficulties have been encountered in obtaining solutions mainly because of the nonlinear inertia terms in the momentum equation.

The various methods which have been used may be placed into one of four categories:

1. Integral:

An early analysis of the hydrodynamic entrance region of a tube and duct was presented by Schiller (*1*). The cross section of the tube or duct was considered to be composed of two regions; a boundary layer developing near the wall and an invicid fluid core. A parabolic velocity distribution was assumed in the boundary layer and Bernoulli's equation was used in the core to determine the pressure distribution in the axial direction. Modifications of this basic method have been subsequently presented elsewhere (*2* to *4*).

2. Axially patched solutions:

In this method, initially used by Schlichting (*5*), the entrance region is divided into two regions. Near the entrance a boundary layer model is used and an approximate solution is obtained in terms of a perturbation of Blasius' boundary layer solution. In the region where the flow is nearly fully developed, the velocity profile is approximated in terms of a small perturbation to the fully developed velocity profile. The two solutions are patched at some appropriate axial location. More recent works (*6* to *10*) have been based upon this method.

3. Linearization of the momentum equation:

The nonlinear inertia terms in the momentum equation were linearized and the solution to the resulting equation found in a method proposed by Langhaar (*11*). Subsequent refinements of this method have been presented elsewhere (*12* and *13*).

4. Finite difference methods:

The boundary layer equations were solved by finite difference methods for flow inside tubes (*3*, *14*), and for parallel plate channels (*15*, *16*).

Several recent publications have described the use of finite difference methods for the flow model considering the axial transport of vorticity and a pressure gradient in the radial as well as axial direction. Vrentas, et al. (*17*) assumed a stream tube to extend from the entrance of the real tube to minus infinity where the axial velocity was considered to be uniform. Schmidt and Zeldin (*18*) assumed the profile to be uniform and the flow irrotational at the tube entrance. Wang and Longwell (*19*) solved the parallel plates channel problem using both the stream tube and uniform entrance velocity inlet conditions. All of these solutions assume fully developed flow at infinity.

One of the major interests in developing flow work is associated with the ability to predict the pressure drop between any two axial locations. In order to facilitate the computations, the total pressure drop from the entrance is expressed as the sum of the pressure drop which would occur if the flow were fully developed for the total length plus a correction factor to account for the developing flow region:

$$\frac{P_o - P_Z}{\frac{pv^2_m}{2}} = fZ + K \tag{1}$$

where f is the fully developed friction factor; $f = 64/N_{Re}$ for a tube and $96/N_{Re}$ for a parallel plate channel and Z is the nondimensional axial distance from the tube entrance, z/D_h. The entrance region pressure drop coefficient is denoted by K and is a function of axial position reaching an asymptotic value as the flow becomes fully developed.

In this study the complete set of Navier-Stokes equations were solved using finite difference techniques. The continuity and momentum equations were put into nondimensional form and the stream function and vorticity were introduced to reduce the number of equations and eliminate the pressure terms. An axial transformation of the type

$$S = 1 - \frac{1}{1 + CZ} \tag{2}$$

was used where C is an arbitrary positive constant. The spatial domain was subdivided into a system of 40 equal subdivisions in the S direction. For the parallel plate channel 40 equal subdivisions were used in the transverse direction. In order to obtain a finer grid near the wall of the tube, a logarithmic type of subdivision was used, again having 40 subdivisions.

The finite difference representations of the differential equations for the vorticity and the stream function at each node in the system were formed using Allen's method (*22*). The solutions to the resulting set of difference equations were obtained using a successive over relaxation method. Once the distributions of the vorticity and stream function are known the velocities are found using the relationships between the velocities and the derivatives of the stream function. The appropriate derivatives of the stream function at each node were determined by differentiating the expressions for the stream function employed in the formation of the difference equations. The nondimensional pressure gradients were determined using the two momentum equations and numerical integration was employed to determine the nondimensional pressure distribution.

Computations were made with three Reynolds numbers, 10,000, 500, and 100. Since the boundary layer assumptions are valid for flows with high Reynolds number, the results for a Reynolds number of 10,000 approach those of a boundary layer solution and hence are directly comparable with previously published solutions. The value of C in Equation (2) was selected so that the centerline velocity at the last interior node in the axial direction was approximately 99% of that for fully developed flow.

The present analysis yields pressure variations in both the axial and transverse directions. The transverse pressure distribution is dependent upon axial location and Reynolds number. The pressure distributions in a tube at the entrance and a location downstream are shown in Figure 1. As the value of Z/N_{Re} increases, the pressure variation in the transverse direction approaches zero for all Reynolds numbers. Due to the presence of this transverse pressure gradient in the entrance region, a modification in the expression for the pressure drop was necessary:

$$\frac{P_o - \overline{P}_z}{\dfrac{\rho v^2_m}{2}} = fZ + \overline{K} \qquad (3)$$

where $\overline{P}$ is the area integral average pressure at a specified axial location, P_o is the centerline pressure at the tube or channel's entrance and $\overline{K}$ is the entrance pressure drop coefficient. The results for $\overline{K}$ are shown in Figures 2 and 3. The dependency of the results upon the Reynolds number is clearly indicated in these figures.

It is appropriate to comment on several points at this time. The continuity and Navier-Stokes equations used in this analysis form an elliptic system of differential equations. As such, the solution in terms of stream function and vorticity depends upon the boundary conditions employed. Neither the mathematical model of the present study nor the stream tube extension model used by Vrentas, et al. (*17*) completely describes the actual flow situation. The discrepancy arises at the entrance, $Z = 0$. However, for moderate and high Reynolds numbers, the irrotational uniform velocity assumption is a generally accepted approximation for the conditions produced by a sudden contraction into a well-rounded entrance. As the Reynolds number decreases, the flow at the tube entrance becomes increasingly dependent upon flow configuration upstream of the entrance and may deviate considerably from the assumed conditions. The results presented for predicting the pressure drop in a system must, therefore, be used with caution when being applied to a low Reynolds number flow. In order to obtain more accurate results under this condition, it becomes necessary to include that portion of the upstream region on whose boundaries the stream function and vorticity conditions are known. The solution may then be obtained by solving the appropriate finite difference equations for the combined regions.

In Table 1 the asymptotic values of K are compared with previously reported results. Values of K for arbitrary cross sections have been presented elsewhere (*20, 21*). As can be seen, the value of K depends to a large extent upon the method of solution used. Integral techniques generally yield lower values. A comparison of the results of this study with those previously obtained using numerical techniques and the boundary-layer assumptions indi-

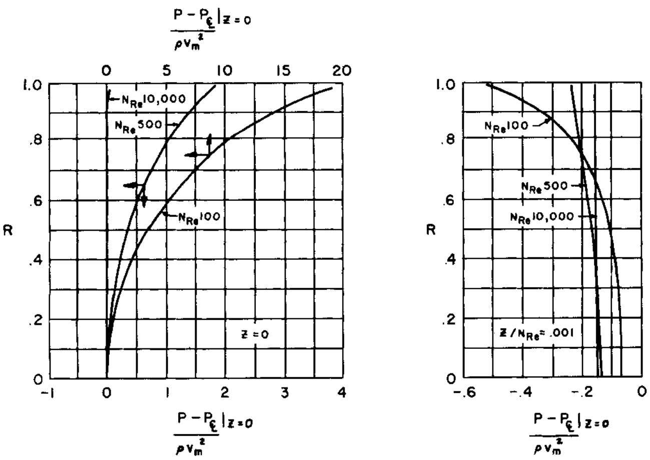

Fig. 1. Nondimensional pressure distribution.

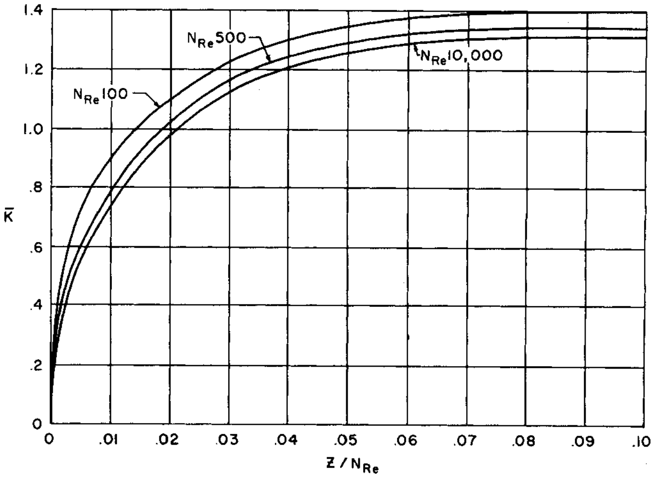

Fig. 2. Tube pressure drop coefficient, $\overline{K}$.

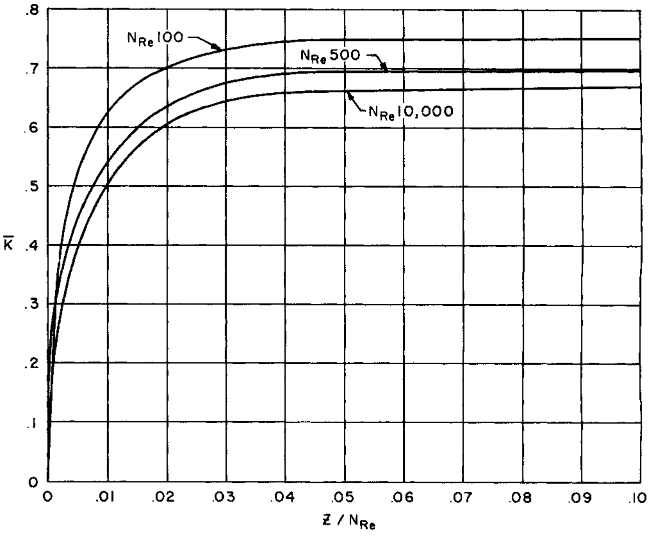

Fig. 3. Parallel plate channel pressure drop coefficient, $\overline{K}$.

TABLE 1. ENTRANCE PRESSURE DROP COEFFICIENT, K (ASYMPTOTIC VALUES)

Tubes

Theoretical	Type of Solution		K
Christianson-Lemmon (*3*)	numerical		1.274
Atkinson-Goldstein (*6*)	patched		1.41
Bogue (*3*)	integral		1.16
Collins-Schowalter (*7*)	patched		1.33
Hornbeck (*14*)	numerical		1.269
Langhaar (*11*)	linearization		1.28
McComas (*21*)	linearization		1.33
Schiller (*1*)	integral		1.16
Present study	numerical	(N_{Re} = 10,000)	1.314
		(N_{Re} = 500)	1.346
		(N_{Re} = 100)	1.397
Siegel (cubic) (*23*)	integral		1.08
Siegel (parabolic) (*23*)	integral		1.106
Sparrow, Lin, and Lundgren (*13*)	linearization		1.24
Tomita (*24*)	linearization		1.22
Vrentas, Duda, and Bargeron (*17*)	numerical (boundary layer)		1.18
Experimental			
Dorsey (*3*)			1.0-1.08
Nikuradse (*25*)			1.32
Rieman (*26*)			1.22-1.268
Schiller (*1*)			1.116-1.450
Weltmann and Keller (*27*)			1.08-1.32

Parallel Plate Channel

Theoretical	Type of Solution		K
Bodoia and Osterle (*15*)	numerical		0.676
Collins and Schowalter (*8*)	patched		0.676
Collins and Schowalter (*7*)	patched		0.740
Ham (*28*)	linearization		0.85
Heaton (*25*)	linearization		0.68
Hwang and Fan (*16*)	numerical		0.625
McComas (*21*)	linearization		0.6857
Roidt and Cess (*10*)	integral		0.630
Schlichting (*5*)	integral		0.601
Present study	numerical	(N_{Re} = 10,000)	0.669
		(N_{Re} = 500)	0.698
		(N_{Re} = 100)	0.748
Sparrow, Lin, and Lundgren (*13*)	linearization		0.686

cate good agreement with results reported (*3, 14*), whereas a significant difference does exist with the results given elsewhere (*17*). These differences may be attributed to the different techniques used in forming the difference equations, the methods of finding the pressure and the fact that the equations describing the flow are different. The boundary-layer assumptions yield a parabolic system of differential equations whereas the system of equations used in this study is elliptic.

LITERATURE CITED

1. Schiller, L., Z. *Angew. Math. Mech.*, **2**, 96 (1922).
2. Shapiro, A. H., Siegel, and S. J. Kline, Proc. 2nd U.S. Natl. Congr. Appl. Mech., 733 (1954).
3. Christiansen, E. B., and H. E. Lemmon, *AIChE J.*, **11**, 995 (1965).
4. Campbell, W. D., and J. C. Slattery, *J. Basic Eng.*, **85**, 41 (1963).
5. Schlichting, H., *ZAMM*, **14**, 368 (1934).
6. Goldstein, S., "Modern Developments in Fluid Dynamics," Vol. 1, p. 304, Clarendon Press, Oxford Press, Oxford (1938).
7. Collins, M., and W. R. Schowalter, *AIChE J.*, **9**, 804 (1963).
8. ———, *Phys. Fluids*, **5**, 1122 (1962).
9. ———, *AIChE J.*, **9**, 55 (1942).
10. Roidt, M., and R. D. Cess, *J. Appl. Mech.*, **84**, 171 (1962).
11. Langhaar, H. L., *ibid.*, **64**, 55 (1942).
12. Slezkin, N. A., "Dynamics of Viscous Incompressible Fluid," Gostekhizdat, Moscow (1955).
13. Sparrow, E. M., S. H. Lin, and T. S. Lundgren, *Phys. Fluids*, **7**, 338 (1964).
14. Hornbeck, R. W., *Appl. Sci. Res., Sec. A*, **13**, 224 (1964).
15. Bodoia, J. R., and J. F. Osterle, *ibid.*, **10**, 265 (1961).
16. Hwang, C. L., and L. T. Fan, *ibid., Sec. B*, **10**, 329 (1961).
17. Vrentas, J. S., J. L. Duda, and K. G. Bargeron, *AIChE J.*, **12**, 837 (1966).
18. Schmidt, F. W., and B. Zeldin, *Symposium Fluid Internal Flow*, Pennsylvania State Univ. (1968).
19. Wang, Y. L., and P. A. Longwell, *AIChE J.*, **10**, 323 (1964).
20. Lundgren, T. S., E. M. Sparrow, and J. B. Starr, *J. Basic Eng.*, **86**, 620 (1964).
21. McComas, S. T., *J. Basic Eng.*, **89**, 847 (1967).
22. Allen, D. N. DeG., and R. V. Southwell, *Quart. J. Mech. Appl. Math.*, **8**, Pt 2, 129 (1955).
23. Siegel, R., DSc thesis, Mass. Inst. Tech., Cambridge (1953).
24. Tomita, Y., *Bull. Japan Soc. Mech. Eng.*, **4**, 77 (1961).
25. Prandtl, L., and O. J. Tietjens, "Applied Hydro and Aeromechanics," McGraw-Hill, New York (1934).
26. Rieman, W., *J. Am. Chem. Soc.*, **50**, 46 (1928).
27. Weltmann, R. N., and T. A. Keller, *Natl. Advisory Comm. Aeron., TN 3889* (1957).
28. Ham, L. S., *J. Appl. Mech.*, **82**, 403 (1960).
29. Heaton, H. S., W. C. Reynolds, and W. M. Kays, *Rept. No. AHT-5*, Mech. Dept., Stanford Univ., California (1962).